Composites Part B 87 (2016) 33–39

Contents lists available at ScienceDirect

Composites Part B

journal homepage: www.elsevier.com/locate/compositesb

On the isotropy of randomly generated representative volume elements for fiber-reinforced elastomers

F. López Jiménez

Department of Civil and Environmental Engineering, Massachusetts Institute of Technology, Cambridge, MA 02139, USA

ARTICLE INFO

Article history:
Received 9 April 2015
Received in revised form
14 September 2015
Accepted 20 October 2015
Available online 30 October 2015

Keywords:
A. Fibres
B. Mechanical properties
C. Finite element analysis (FEA)
C. Statistical properties/methods
Soft composites

ABSTRACT

The isotropy of different numerical simulations of fiber reinforced elastomers has been explored by explicitly applying stretch in different loading directions, in models with representative volume elements (RVEs) spanning a wide range of fiber volume fractions and system sizes. The results show that the homogenized response is not the same for all loading directions, and that the corresponding dependance takes the form of a sine. The anisotropy decreases with the RVE size, and so it can be used to asses if the scales can be separated in a given model. Considering the average response over all loading directions greatly reduces the variation between different RVEs, which can be used to improve the accuracy of the simulations in a way that is significantly more efficient than increasing the size of the RVE. The simulations have also shown a good correlation between the isotropy of each representative volume element at low and high values of the applied stretch. The result of linear simulations can therefore be used as an efficient indication of the anisotropy expected at high deformations.

1. Introduction

Fiber-reinforced composites are widely used in industry due to their high stiffness-to-weight and strength-to-weight ratio. In addition to their application as structural elements, in recent years new elastomer-based composites have been proposed in systems that exploit the mechanics of large deformations, with examples ranging from strain sensing [32] to deployable structures [18] and shape memory composites [7]. This new set of constituent materials, loading conditions and application requirements have made necessary the development of new tools to predict the mechanical response of fiber composites in the nonlinear regime [27].

A set of such tools are analytical homogenization techniques. Following the pioneering work of Ponte Castañeda [26], several studies have provided increasingly refined homogenization models for the nonlinear behavior of fiber-composites [3,4,21,1,20]. However, this is a very complicated problem, where the possibility of obtaining simple closed form solutions is limited to a certain set of constituents and microstructure geometries. In addition, such models can only provide the homogenized response, and are unable to study the microscopic strain and stress fields.

The other option is numerical-based homogenization [22], which is widely used in the study of both linear and nonlinear composites [10,13,2,31]. This approach is based on the existence of a representative volume element (RVE) in which the microstructure and size are such that its overall response is the same as that of the real material. This is called separation of scales between the microscopic and macroscopic scales, and is only strictly true in the case in which the size of the RVE is mathematically infinite, that is, extremely large compared to the fiber dimension. The main problem is, therefore, establishing the minimum element size that provides a sufficiently accurate prediction of the response of the ideal composite, as well as bounding the associated error [28]. Several authors have provided estimates for this critical size in the case of composites with linearly elastic properties [5,11,14]. In the case of nonlinear composites, the critical size of the RVE depends not only on the source of nonlinearity, but also on the criteria used to establish if the different realizations of the RVE, with increasing size, have converged to the behavior of the ideal, infinite composite [15,30,25,8,9,23,12], the most common being the convergence of the homogenized mechanical response, that is, the macroscopic average stiffness, as the model size increases.

Another possible criteria is the requirement that, since a composite of infinite size and random microstructure must be isotropic, the response of the numerical model should be isotropic too. Deviations from this ideal behavior are therefore a numerical artifact

E-mail address: flopezj@mit.edu.

http://dx.doi.org/10.1016/j.compositesb.2015.10.014
1359-8368/

due to the finite size of the model. The RVE size is considered to be sufficiently large, then, when its mechanical response is close to isotropic. This is commonly assessed by looking at the coaxility of the strain and stress tensors [19]. However, and to the author's knowledge, there are no published studies in which the isotropy is explicitly explored by systematically varying the loading direction. This provides a direct measure of the RVE anisotropy, that can be explored as a function of its size and fiber volume fraction. The fact that the level of isotropy of a given microstructure might change as the applied loading increases, as it happens with nonlinear composites, has also seldom been addressed in the existing literature.

The goal of this work is to study the isotropy associated to the RVE size at low and high strains, as well as the relationship between isotropy and convergence of the homogenized response as the size of the RVE increases. We will focus on two-dimensional RVEs, with parallel fibers, that are transversely isotropic in the plane perpendicular to the fiber direction. There are two main reasons to choose this simplified geometry. First, it is a particularly interesting case since the mechanical properties are dominated by the matrix, and the evolution of the fiber arrangement as the loading increases significantly affects the nonlinear response. Second, we will make use of the fact that the response of an incompressible material under plane strain can be defined with only two parameters, namely the principal stretch, λ, and the angle of the corresponding principal direction, θ, in order to explicitly explore the isotropy of the RVEs: for all realizations of our model, the same value of λ will be applied at several values of θ, which provides the homogenized stiffness as a function of the loading direction. The numerical model will be presented in Section 2. The results for small and large strain loading will be presented in Section 3, followed by a summary and discussion of the main findings in Section 4.

2. Computational model

Numerical homogenization is performed through a series of finite element simulations with the commercial package Abaqus. The RVEs are loaded applying a macroscopic deformation gradient $\overline{\mathbf{F}}$ through a combination of dummy nodes and periodic boundary conditions. The total strain energy of each RVE is used to calculate a homogenized strain energy density $\overline{W}$:

$$\overline{W} = \frac{\int_{A_f} W_f dA_f + \int_{A_m} W_m dA_m}{A_f + A_m} \tag{1}$$

where W_i and A_i are the strain energy density and area of either fiber, f, and matrix, m. The rest of this section provides details on the parameters, microstructure and boundary conditions of the model. A very similar model has been verified with experimental results of carbon fiber composites with a soft silicone matrix [17].

2.1. Geometrical and material parameters

We consider an idealized composite with cylindrical fibers of radius r, extending perfectly parallel in the X_1 direction and with a random distribution within the X_2–X_3 plane. The composite is therefore transversely isotropic, i.e. isotropic in the plane perpendicular to the fiber direction. The fiber volume fraction is V_f. In the simulations presented here we assume plane strain to reduce the geometry to a square two-dimensional RVE of side length $L_2 = L_3 = \delta r$, with $N_f = V_f \delta^2/\pi$ fibers. Assuming generalized plane strain yields the same results, since the extreme stiffness of the fibers with respect to the matrix prevents any stretching in the X_1 direction. A schematic of the model is shown in Fig. 1.

Both fiber and matrix are modeled as incompressible hyperelastic Neo-Hookean materials, with strain energy density $W_i = \mu_i/2(I_1-3)$, where μ_i is the linear shear stiffness of the component i and I_1 is the first invariant of the Cauchy-Green deformation gradient $\mathbf{C} = \mathbf{F}'\mathbf{F}$, defined in function of the principal stretches λ_i as $I_1 = \sum_{i=1}^{3} \lambda_i^2$ [24]. The bonding between both components is assumed to be perfect. The ratio of stiffness between fibers and matrix is taken so that the fibers behave as rigid, $\mu_f/\mu_m = 10000$. Linear quadrilateral elements CPE4H are used for both components, with hybrid formulation to account for incompressibility. An average element size of $0.1r$ has been chosen after a parametric mesh size study.

2.2. Boundary conditions and loading

Periodic boundary conditions are applied in all faces of the RVE using the command EQUATION in Abaqus. This requires the mesh to be identical in all opposite faces of the RVE. The conditions can be summarized as:

$$\begin{aligned} \mathbf{u}(L_2, X_3) - \mathbf{u}(0, X_3) &= \overset{2}{\mathbf{u}} \\ \mathbf{u}(X_2, L_3) - \mathbf{u}(X_2, 0) &= \overset{3}{\mathbf{u}} \end{aligned} \tag{2}$$

where $\overset{i}{u}_j = \overline{F}_{ij} L_j$, L_j is the length of the RVE in the j-th direction, and $\overline{\mathbf{F}}$ is the applied deformation gradient, $\overline{F}_{ij} = \partial x_i/\partial X_j$. Using the spectral theorem, the Cauchy-Green deformation gradient can be expressed as a function of the principal stretches λ_i and principal directions $\mathbf{n_i}$ as

$$\mathbf{C} = \sum_{1}^{3} \lambda_i \mathbf{n_i} \otimes \mathbf{n_i} \tag{3}$$

The condition of plain strain imposes $\lambda_1 = 1$, $\mathbf{n}_1 = [1\ 0\ 0]$. The additional restraint due to incompressibility implies that all possible deformations are defined by a single principal stretch, $\lambda_2 = 1/\lambda_3 = \lambda$, and a direction θ, $\mathbf{n}_1 = [0 \quad \cos\theta \quad \sin\theta]$ and $\mathbf{n}_2 = [0 \quad -\sin\theta \quad \cos\theta]$. Equation (3) is then used to calculate $\mathbf{C}$, and the deformation gradient is obtained solving the equation $\mathbf{F}'\mathbf{F} = \mathbf{C}$.

The components of $\overset{i}{\mathbf{u}}$ can therefore be obtained from the desired principal stretch and direction, and imposed to the model through auxiliary dummy nodes. However, imposing the four displacements often leads to numerical errors, since even small rounding errors result in a violation of the incompressibility condition. In practice, this is resolved by allowing free expansion in the X_3 direction. Analysis of the results show that the resultant displacement is basically equal to $F_{33}L_3$, as expected.

2.3. Fiber arrangement

For a given set of values of δ and V_f, the microstructure is fully described by the position of the center of the fibers within the RVE. These are obtained through a random sequential adsorption algorithm [6]. This is is a hard-core process, i.e. a Poisson process in which a limitation on the minimum distance between the centers is introduced: the positions are obtained randomly, and rejected if the distance to any of the already allocated fibers is less than a given limit. In this work, an unless noted otherwise, the minimum distance adopted is 1.1 times the diameter. Additionally, a fiber is also rejected if the distance between its center to the edge of the RVE is in the $[0.9r, 1.1r]$ interval. The goal of both conditions is creating a geometry that can be easily meshed.

It is possible that a given fiber distribution reaches a jammed configuration [29], in which no new fibers can be added without violating the non-overlap restriction. For this reason, if after 1000

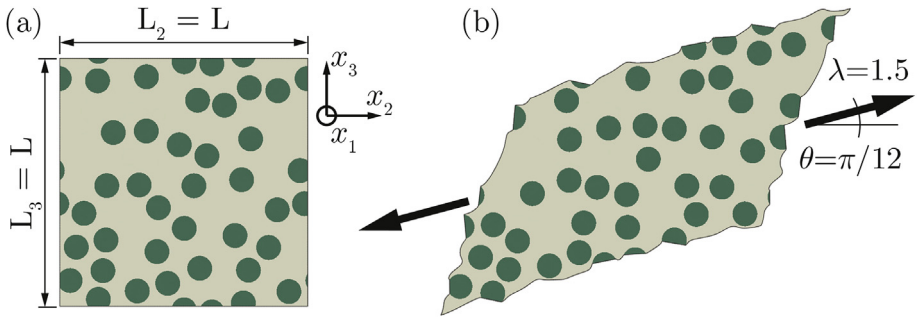

Fig. 1. Representative volume element (RVE) in the (a) undeformed and (b) deformed configuration. The example has $V_f = 0.3$ and $\delta = 30$, and the loading is characterized by $\lambda = 1.5$ and $\theta = \pi/12$.

attempts a new fiber has not been accepted, the microstructure is discarded and the algorithm starts from zero.

3. Results

The results will be presented using the ratio between homogenized strain energy density of the composite and the first invariant of the applied deformation, $\overline{W}/(\overline{I_1} - 3)$. In the small strain regime, this is an approximation of the homogenized shear stiffness, $\overline{\mu}$. This is also true in Neo-Hookean materials at all strains, since $W = \mu(I_1 - 3)$. A previous study [16] has shown that the nonlinear behavior of composites with Neo-Hookean components with moderate fiber concentration is itself very similar to a Neo-Hookean solid, even at moderately high strains. Furthermore, even if the behavior of the composite deviates from a Neo-Hookean material, the ratio provides a simple and physically meaningful description of the response.

Four different values of both the volume fraction, V_f, and the size parameter, $\delta = r/L$, have been used in the present study. For each combination of the two, ten different realizations of the microstructure are created, and for each model the loading direction θ is varied in the range $\theta = [0,\pi]$, as summarized in Fig. 2. The results are presented as statistical quantities at two different levels. First, the anisotropy of a particular RVE is given by the mean or expected value (E_θ), standard deviation (SD_θ) and coefficient of variation ($CV_\theta = E_\theta/SD_\theta$) of the response over a given interval of θ. Once the response of each RVE is identified, it is then possible to consider the mean and coefficient of variation within different RVEs of the same size and volume fraction, E_{RVE} and CV_{RVE} respectively.

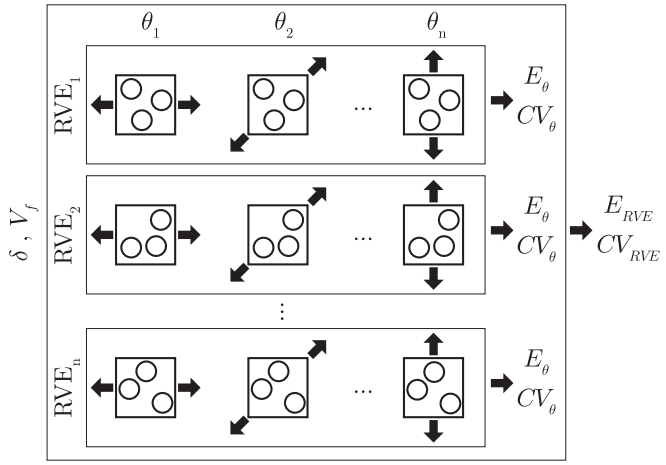

Fig. 2. Schematic of the process followed to obtain statistics of the results. For each RVE size and volume fraction, several realizations have been created. For each realization, RVE_i, the loading is applied in different directions. The corresponding average and coefficient of variations are E_θ and CV_θ. The average and variation over all the RVEs with the same size and volume fraction is given by E_{RVE} and CV_{RVE}.

Table 1
Number of fibers for the values of δ and V_f considered in the study.

		V_f			
		0.1	0.2	0.3	0.4
δ	10	3	6	10	13
	20	13	25	38	51
	30	29	57	86	115
	40	51	102	153	204

It should be noted that the values of L used in the study are not exactly equal to δr, but the closest value giving an integer number of fibers, so that the fiber volume fraction is strictly enforced. Table 1 summarizes the geometries considered; for each combination of V_f and δ, ten different realizations of the RVE have been created and studied. An example of a simulation is shown in Fig. 3, corresponding to a RVE with $V_f = 0.3$ and $\delta = 30$. The applied loading is $\lambda = 1.5$ and $\theta = \pi/4$.

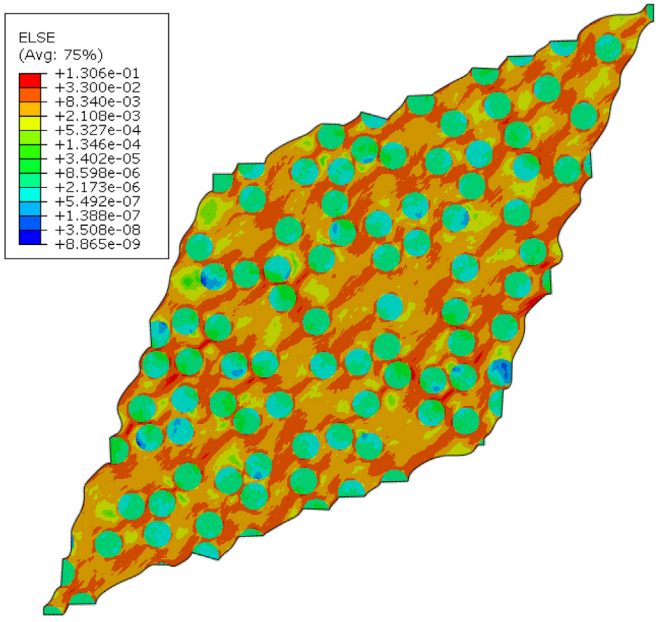

Fig. 3. Example of Abaqus simulation with $V_f = 0.3$ and $L = 30$, with loading $\lambda = 1.5$ in the direction $\theta = \pi/4$. Color represents the strain energy density, as a multiple of the shear modulus of the matrix, μ_m.

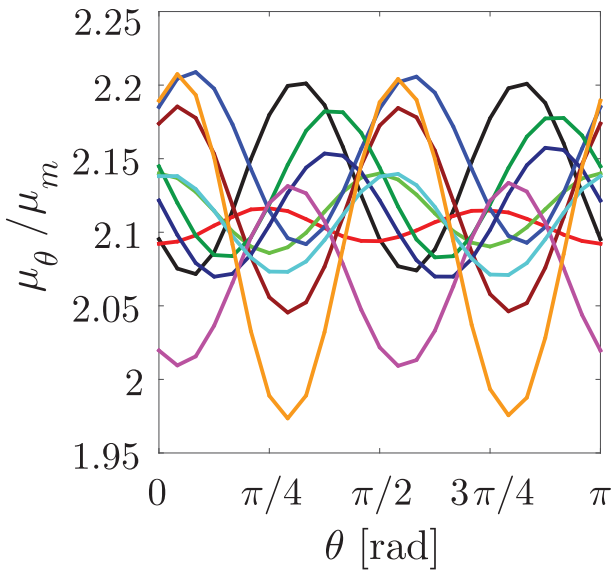

Fig. 4. Response to a deformation of $\lambda = 1.01$ as a function of the loading angle θ for the ten different realizations with $V_f = 0.3$, $\delta = 30$.

3.1. Linear response

A first set of results have been obtained applying a deformation of $\lambda = 1.01$, which in the case of a composite with Neo-Hookean components is within the initial linear regimen. We can calculate the initial shear stiffness μ_θ as a function of the direction of the applied loading, θ, which in all cases can be expressed as $\mu_\theta = \widetilde{\mu} + \Delta\mu \sin(4\theta + \theta_0)$. The values of the mean shear stiffness, $\widetilde{\mu}$, the amplitude of the variation, $\Delta\mu$, and the phase, θ_0, vary within different RVEs with identical sizes and concentrations, see Fig. 4.

For each of the different realizations we can calculate the mean or expected value (E_θ), standard deviation (SD_θ) and coefficient of variation ($CV_\theta = E_\theta/SD_\theta$) of μ_θ over the interval $\theta = [0,\pi]$. For a sine, the expressions simplify to $E_\theta[\mu_\theta] = \widetilde{\mu}$ and $SD_\theta[\mu_\theta] = \Delta\mu/\sqrt{2}$. The values of θ have been discretized using $\pi/12$ intervals; differences with a discretization in $\pi/24$ intervals, as shown in Fig. 4, are of the order of 1%. It should be noted that, given the sinusoidal dependance with θ, then one simply has that $E[\mu_\theta] = \mu_\gamma + \mu_{\gamma+\pi/4}$, for any value of γ, which greatly reduces the computational cost.

Fig. 5 shows the value of the expected value $E_\theta[\mu_\theta]$ and the coefficient of variation $CV_\theta[\mu_\theta]$ of the response of each of the RVEs considered. As expected, the predicted stiffness converges as the size of the numerical model increases, and the anisotropy of each RVE decreases. The coefficient of variation also shows how the dispersion between different realizations, i.e. the anisotropy, is higher for systems with high fiber density. In both cases there is convergence as δ increases, as expected in a problem with separation of scales.

We consider now that each RVE provides a single prediction of the behavior of the composite, $\widetilde{\mu}_\theta = E_\theta[\mu_\theta]$, which has been obtained taking into account a range of loading directions θ. Our goal is then to obtain an average of this prediction for all realizations of the RVE, $E_{RVE}[\widetilde{\mu}_\theta]$, as well as the corresponding coefficient of variation, $CV_{RVE}[\widetilde{\mu}_\theta]$, which describes the variation in response between RVEs with the same fiber volume fractions and size. It is particularly interesting to compare the prediction considering the full variation of angle $\theta = [0,\pi]$, with predictions obtained considering only the loading in a single direction, that is, for a given value of θ. Fig. 6 shows how considering the average response over θ improves the convergence of the response, as well as greatly decreases the variation between different RVEs. This means that the prediction obtained this way will be much more robust with respect to differences in the particular fiber arrangement of the model. Due to the sinusoidal nature of the response, $\widetilde{\mu}_\theta = E_\theta[\mu_\theta]$ can be obtained with just two simulations at γ and $\gamma + \pi/4$, for any γ, a computational cost much smaller than the increase in model size required to achieve the same improvements with a single loading direction. Fig. 6 can also be used as a guideline to choose a RVE size. Although this choice would depend on the given application, it is readily apparent that for dense systems, a system size of $\delta = 20$ already presents a significant reduction in the expected spread between different RVEs.

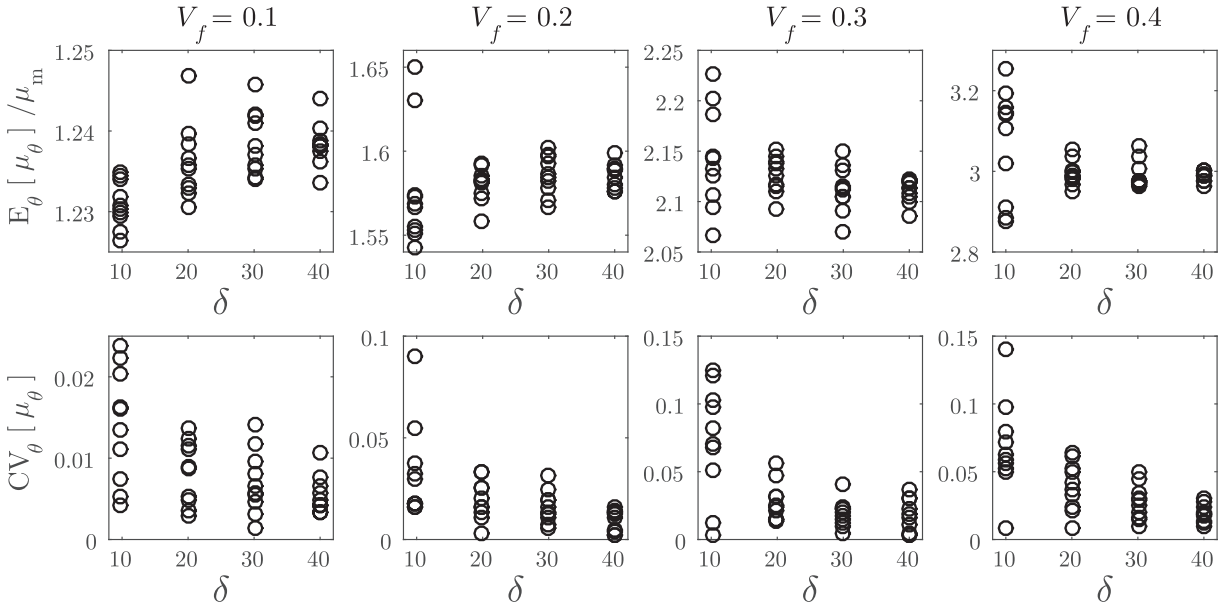

Fig. 5. Expected value $\widetilde{\mu} = E_\theta[\mu_\theta]$ and coefficient of variation $CV_\theta[\mu_\theta]$ for all realizations of RVEs with fiber volume fraction V_f and size δ.

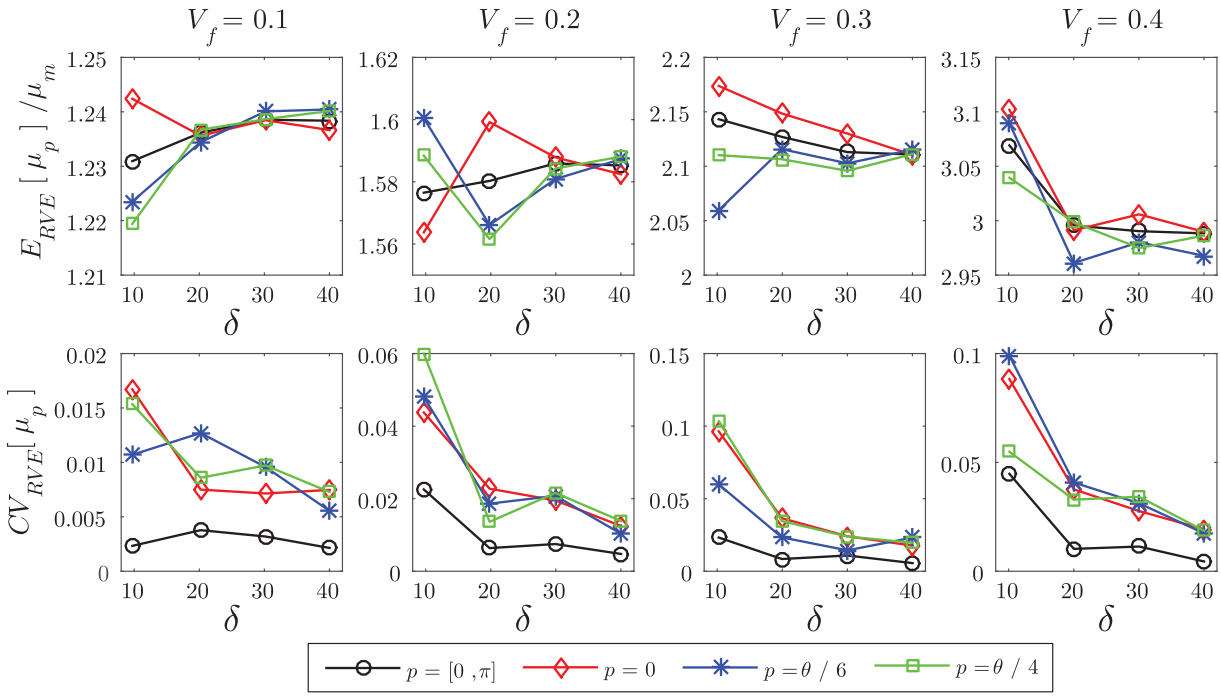

Fig. 6. Expected value $E_{RVE}[\mu_{\theta_p}]$ and coefficient of variation $CV_{RVE}[\mu_{\theta_p}]$ for different realizations of RVEs with fiber volume fraction V_f and size δ. Each curve has been calculated using a different loading direction, p.

3.2. Nonlinear regime

In order to study the evolution of the anisotropy in the nonlinear regime, we now consider a maximum principal stretch of $\lambda = 1.5$, applied over the same range of directions θ. This value has been chosen as being the maximum deformation in which the cases with $V_f = 0.4$ converge without the need of numerical techniques such as remeshing or numerical viscous damping, which could affect the response by a small but noticeable amount. It is also sufficient for possible practical applications, since it is well beyond the failure stretch observed experimentally in fiber reinforced elastomers [17]. In this case the response is simply defined as $\overline{W}/(\overline{I_1} - 3)$, since at hight strains the response might deviate from that of a Neo-Hookean material [16].

Fig. 7 shows the response of all RVEs with $V_f = 0.3$ and $\delta = 30$ when the applied deformation is $\lambda = 1.5$, as a function of the loading direction θ. In this case the anisotropy no longer takes the form of a sine with respect to θ, although some similarities can be observed with the response at $\lambda = 1.01$ for the same RVEs presented in Fig. 4.

The evolution of the response as the loading increases is shown in Fig. 8, a comparison of expected value and coefficient of variation of the homogenized response for all realizations of the RVEs, E_{RVE} and CV_{RVE}, for three different values of the applied stretch λ. For all parameters the response at different loading stages are very similar, both in the expected value and in the variation between different RVEs. Again, a significant decrease in the coefficient of variation is observed after $\delta = 20$, specially for systems with a dense concentration of fibers.

We now compare the anisotropy of each individual RVE at small and high strains, characterized in both cases by the corresponding coefficient of variation over the loading direction, $CV_\theta[\mu_\theta]$ and $CV_\theta[\overline{W}/(\overline{I_1} - 3)]$, respectively. A close relationship between the two would make it possible to predict anisotropy at high strains using simulations in the linear regime. This is a computationally very efficient way to evaluate the suitability of a given realization of the RVE, particularly since at low strains the coefficient of variation can be calculated with just two simulations, thanks to the sinusoidal dependance on θ, which is no longer true for high values of the stretch. Fig. 9 shows how the coefficient of variation at $\lambda = 1.01$ and $\lambda = 1.5$ are reasonably correlated for all values of V_f and δ, with a Pearson's coefficient of 0.84, which means that an analysis in the linear regime is a good indication of the anisotropy expected a high deformations. Furthermore, the figure shows that when large deviations from correlation take place, they consist on cases in which the anisotropy is higher at large strains, so the results for low deformation serve as a useful lower bound.

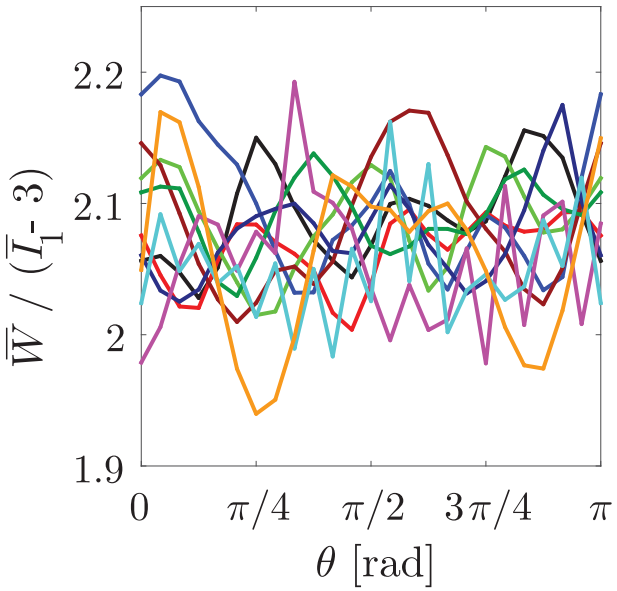

Fig. 7. Response to a deformation of $\lambda = 1.5$ as a function of the loading angle θ for the ten different realizations with $V_f = 0.3$, $\delta = 30$.

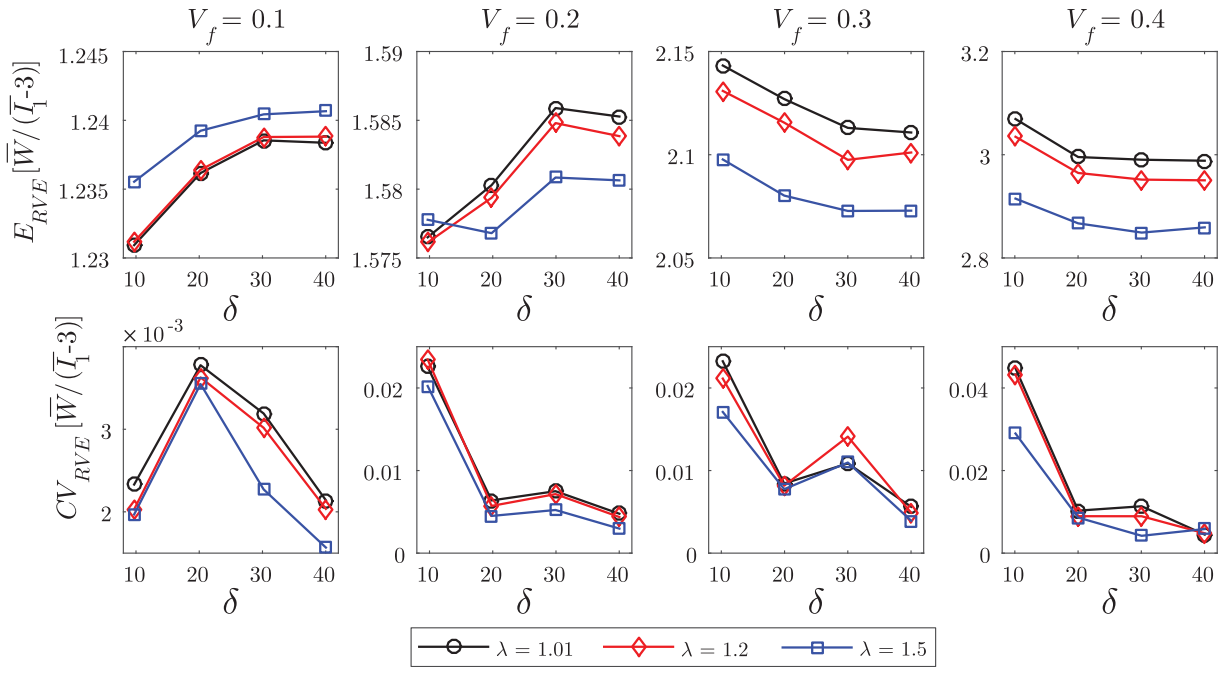

Fig. 8. Expected value $E_{RVE}[\mu_{\theta_p}]$ and coefficient of variation $CV_{RVE}[\mu_{\theta_p}]$ for different realizations of RVEs with fiber volume fraction V_f and size δ. Each curve corresponds to a different loading stretch, λ.

4. Summary and discussion

The isotropy of RVEs for fiber reinforced elastomers has been studied with numerical simulations in which the same stretch has been applied in several different directions. Ten different realizations of different sizes and fiber concentrations have been considered, and in all cases the macroscopic response of the model showed a clear dependance on the loading direction, θ. The variation of the homogenized response over θ has then been used to define the anisotropy of each realization of the RVE.

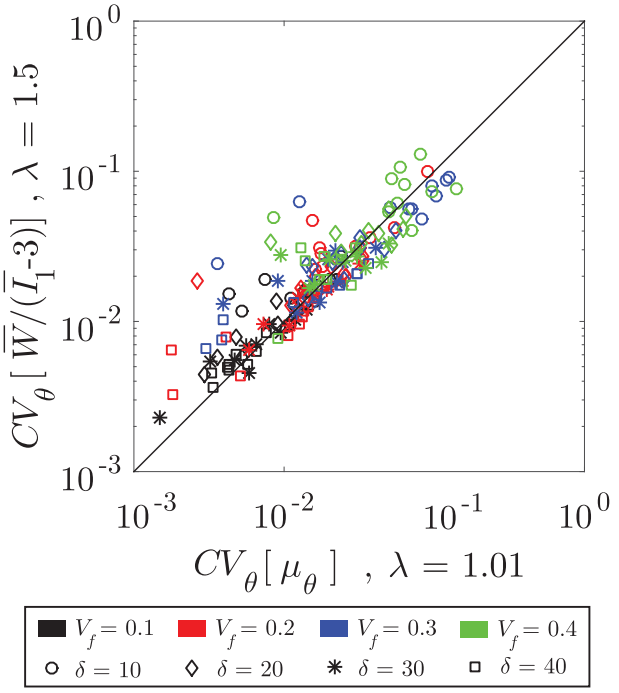

Fig. 9. Coefficient of variation of responses in the linear regime, $\lambda = 1.01$, and the nonlinear regime, $\lambda = 1.5$, over all volume fraction and system sizes. The line corresponds to equal coefficient of variation at both strains. The correlation coefficient is 0.84.

Two main findings have been presented. The first one is the fact that in the linear regime, the response as a function of the loading direction has a sinusoidal shape, and that considering the mean value of such sine provides a prediction for the response of the real composite that is much more robust than that obtained considering the response in a given, fixed direction. This is able to provide a reduction in computational cost, since the expected value of a sine can be calculated using just two loading directions. The evolution of the anisotropy with respect to the system size can also be used to verify that there is separation of scales. Furthermore, the fact that the phase of every sine is different implies that this variation is not purely an effect of the boundary conditions or the way the microstructure of the different RVEs are obtained.

Second, anisotropy in the linear regime correlates reasonably well with the anisotropy in the nonlinear regime. This means that the results from linear simulations can be used to provide a reasonable prediction of the isotropy expected at high deformations, with the subsequent save in computational costs.

The study has made use of the convenient fact that, due to incompressibility, all two-dimensional deformations are equivalent to shear, and can be parameterized by the magnitude of the main principal stretch, λ, and its direction, θ. However, in the case of compressible composites, this is no longer true, since there is no longer an unique relation between the two principal stretches. In this case it will be necessary to consider different deformation modes, such as tension, pure and simple shear or biaxial tension. In particular, it would be interesting to study if the level of isotropy of a given RVE is roughly the same for all loading conditions, or if a given microstructure might show different levels of anisotropy as a function of the loading type.

In addition, the present approach could also be used to study composites with anisotropic behavior, such as the cases of material properties or microstructure dependant on the fabrication process.

In that case it will necessary to compare the anisotropy observed in the numerical model with that expected in the ideal composite.

Acknowledgments

The author would like to thank Prof. Oscar Lopez-Pamies (UIUC) and Prof. Celia Reina (UPenn) for useful discussions.

References

[1] Agoras M, Lopez-Pamies O, Ponte Castañeda P. A general hyperelastic model for incompressible fiber-reinforcedelastomers. J Mech Phys Solids 2009;57. 268286.
[2] Catapano A, Jumel J. A numerical approach for determining the effective elastic symmetries of particulate-polymer composites. Compos Part B Eng 2015;78:227–43.
[3] deBotton G. Transversely isotropic sequentially laminated composites in finite elasticity. J Mech Phys Solids 2005;53:1334–61.
[4] deBotton G, Hariton I, Socolsky E. Neo-hookean fiber-reinforced composites in finite elasticity. J Mech Phys Solids 2006;54:533–59.
[5] Drugan W, Willis J. A micromechanics-based nonlocal constitutive equation and estimates of representative volume element size for elastic composites. J Mech Phys Solids 1996;44:497–524.
[6] Feder J. Random sequential adsorption. J Theor Biol 1980;87:237–54.
[7] Ge Q, Luo X, Rodriguez ED, Zhang X, Mather PT, Dunn ML, et al. Thermomechanical behavior of shape memory elastomeric composites. J Mech Phys Solids 2012;60:67–83.
[8] Gitman I, Askes H, Sluys L. Representative volume: existence and size determination. Eng Fract Mech 2007;74:2518–34.
[9] González C, LLorca J. Mechanical behavior of unidirectional fiber-reinforced polymers under transverse compression: microscopic mechanisms and modeling. Compos Sci Technol 2007;67:2795–806.
[10] Greco F, Luciano R. A theoretical and numerical stability analysis for composite micro-structures by using homogenization theory. Compos Part B Eng 2011;42:382–401.
[11] Gusev AA. Representative volume element size for elastic composites: a numerical study. J Mech Phys Solids 1997;45:1449–59.
[12] Heinrich C, Aldridge M, Wineman A, Kieffer J, Waas A, Shahwan K. The influence of the representative volume element (rve) size on the homogenized response of cured fiber composites. Model Simul Mater Sci Eng 2012;20: 075007.
[13] Kamiński M. Homogenization with uncertainty in poisson ratio for polymers with rubber particles. Compos Part B Eng 2015;69:267–77.
[14] Kanit T, Forest S, Galliet I, Mounoury V, Jeulin D. Determination of the size of the representative volume element for random composites: statistical and numerical approach. Int J solids Struct 2003;40:3647–79.
[15] Khisaeva Z, Ostoja-Starzewski M. On the size of rve in finite elasticity of random composites. J Elast 2006;85:153–73.
[16] López Jiménez F. Modeling of soft composites under three-dimensional loading. Compos Part B Eng 2014;59:173–80.
[17] López Jiménez F, Pellegrino S. Constitutive modeling of fiber composites with a soft hyperelastic matrix. Int J Solids Struct 2012a;49:635–47.
[18] López Jiménez F, Pellegrino S. Folding of fiber composites with a hyperelastic matrix. Int J Solids Struct 2012b;49:395–407.
[19] Lopez-Pamies O, Goudarzi T, Danas K. The nonlinear elastic response of suspensions of rigid inclusions in rubber: Iia simple explicit approximation for finite-concentration suspensions. J Mech Phys Solids 2013;61:19–37.
[20] Lopez-Pamies O, Idiart MI. Fiber-reinforced hyperelastic solids: a realizable homogenization constitutive theory. J Eng Math 2010;68:57–83.
[21] Lopez-Pamies O, Ponte Castañeda P. On the overall behavior, microstructure evolution, and macroscopic stability in reinforced rubbers at large deformations: II - application to cylindrical fibers. J Mech Phys Solids 2006;54: 831863.
[22] Michel J, Moulinec H, Suquet P. Effective properties of composite materials with periodic microstructure: a computational approach. Comput methods Appl Mech Eng 1999;172:109–43.
[23] Moraleda J, Segurado J, LLorca J. Finite deformation of incompressible fiber-reinforced elastomers: a computational micromechanics approach. J Mech Phys Solids 2009;57:1596–613.
[24] Ogden R. Non-linear elastic deformations. Courier Corporation; 1997.
[25] Ostoja-Starzewski M, Du X, Khisaeva Z, Li W. Comparisons of the size of the representative volume element in elastic, plastic, thermoelastic, and permeable random microstructures. Int J Multiscale Comput Eng 2007;5.
[26] Ponte Castañeda P. The effective mechanical properties of nonlinear isotropic composites. J Mech Phys Solids 1991;39:45–71.
[27] Ponte Castañeda P, Suquet P. Nonlinear composites. Adv Appl Mech 1998;34: 171–302.
[28] Suquet P. Elements of homogenization for inelastic solid mechanics. Homog Tech Compos media 1987;272:193–278.
[29] Tanemura M. On random complete packing by discs. Ann Inst Stat Math 1979;31:351–65.
[30] Trias D, Costa J, Turon A, Hurtado J. Determination of the critical size of a statistical representative volume element (srve) for carbon reinforced polymers. Acta Mater 2006;54:3471–84.
[31] Tsalis D, Chatzigeorgiou G, Charalambakis N. Homogenization of structures with generalized periodicity. Compos Part B Eng 2012;43:2495–512.
[32] Zhu J, Wei S, Ryu J, Guo Z. Strain-sensing elastomer/carbon nanofiber metacomposites. J Phys Chem C 2011;115:13215–22.